

- ¹F. K. Fong, Phys. Rev. **187**, 1099 (1969).
- ²R. H. Heist and F. K. Fong, Phys. Rev. B **1**, 2970 (1970).
- ³F. K. Fong and E. Y. Wong, Phys. Rev. **162**, 348 (1967).
- ⁴F. K. Fong, R. H. Heist, C. R. Chilver, J. C. Bellows, and R. L. Ford, J. Luminescence **2**, 823 (1970).
- ⁵F. K. Fong, Phys. Rev. B **1**, 4157 (1970).
- ⁶F. K. Fong and J. C. Bellows, Phys. Rev. B **1**, 4240 (1970).
- ⁷F. K. Fong and J. C. Bellows, Phys. Rev. B **2**, 2636 (1970).
- ⁸B. R. Judd, *Operator Techniques in Atomic Spectroscopy* (McGraw-Hill, New York, 1963), Chap. 2.
- ⁹W. E. Bron and W. R. Heller, Phys. Rev. **136**, A1433 (1964).
- ¹⁰M. J. Weber, Phys. Rev. **171**, 283 (1968).
- ¹¹W. B. Gandrud and H. W. Moos, J. Chem. Phys. **49**, 2170 (1968).
- ¹²L. A. Riseberg and H. W. Moos, Phys. Rev. **174**, 429 (1968).
- ¹³L. G. Van Uitert, E. F. Dearborn, and W. H. Grodkiewicz, J. Chem. Phys. **49**, 4400 (1968).
- ¹⁴F. K. Fong, J. A. Cape, and E. Y. Wong, Phys. Rev. **151**, 299 (1966).
- ¹⁵R. Venkataraghavan, F. McLafferty, and J. Amy, Anal. Chem. **39**, 178 (1967).
- ¹⁶G. D. Watkins, Phys. Rev. **113**, 79 (1959); **113**, 91 (1959).

Experimental and Theoretical Study of the Low-Lying Energy-Level Structure of Sm^{3+} in CaF_2

H. Nara* and M. Schlesinger

Department of Physics, University of Windsor, Windsor 11, Ontario, Canada

(Received 3 August 1970)

The optical spectrum exhibited by the Sm^{3+} ion in CaF_2 is analyzed assuming both octahedral and trigonal site symmetries. Calculations were performed using a tensor operator technique in the complete intermediate-coupling scheme. The crystal field parameters and the root-mean-square (rms) deviations obtained are $B^{(4)} = -906 \text{ cm}^{-1}$ and $B^{(6)} = 618 \text{ cm}^{-1}$, with rms deviations of 48.1 cm^{-1} for the octahedral site symmetry; $B_0^{(2)} = 118 \text{ cm}^{-1}$, $B_0^{(4)} = -272 \text{ cm}^{-1}$, $B_3^{(4)} = -296 \text{ cm}^{-1}$, $B_0^{(6)} = 38 \text{ cm}^{-1}$, $B_4^{(6)} = -128 \text{ cm}^{-1}$, and $B_6^{(6)} = 1556 \text{ cm}^{-1}$, with rms deviation of 35.4 cm^{-1} for the trigonal site symmetry. It is suggested that the sample on which the measurements were carried out contains Sm^{3+} ions occupying both octahedral and trigonal symmetry sites. It is also shown that crystal field theory with a single set of $B_q^{(k)}$ parameters is quite adequate to describe the energy levels lying below $11\,000 \text{ cm}^{-1}$, above which a fairly large energy gap follows.

I. INTRODUCTION

The optical absorption, fluorescence, and paramagnetic resonance spectra of Sm^{3+} in CaF_2 have been investigated by several authors.¹⁻³ In particular, Rabiner² investigated the fluorescence of Sm^{3+} in CaF_2 at tetragonal site symmetry and gave a theoretical interpretation.

The $\text{CaF}_2:\text{Sm}^{3+}$ system is of special interest as the strength of the crystal field is believed to be comparable to that of the spin-orbit interaction. This situation suggests that, in analyzing the experimental spectra, one should treat the system on the basis of the complete intermediate-coupling scheme. Fortunately, very accurate free-ion energy eigenvectors⁴ are now available, and this treatment is possible in principle. This treatment, however, requires that very large matrices be diagonalized.

A fairly large energy gap of about 7500 cm^{-1} separates the lower-lying levels from higher ones. Crystal field matrix elements between the lower and upper groups of levels are small compared with the gap of 7500 cm^{-1} , and may be neglected. The

lower group of levels may then be treated separately. Therefore one can work with matrices of considerably smaller dimensions, enabling one to perform the calculations of the type above.

Since the Sm^{3+} ion substitutes for Ca^{2+} ions in the CaF_2 crystal, there must be some kind of charge compensator so as to preserve charge neutrality. The actual site symmetry of the Sm^{3+} in the CaF_2 matrix will depend on the charge compensation mechanisms, which in turn depend on type and amount of impurities, growing conditions, thermal history, etc. Three main site symmetries⁵ are possible for Sm^{3+} in CaF_2 , namely, octahedral (O_h), tetrahedral (C_{4v}), and trigonal (C_{3v}) symmetries. Careful study of the influence of heat treatments³ along with theoretical calculations enables one to classify the lines in the spectra according to their site symmetries. The heat treatment technique, however, is not practical for absorption lines lying below about $11\,000 \text{ cm}^{-1}$ because of opaque milkiness which is introduced in the crystals as a result of heat treatment. In this paper, where we are primarily concerned with the energy region up to $11\,000 \text{ cm}^{-1}$, we shall at-

tempt to analyze the spectra in "as received" Harshaw crystals assuming the three most probable site symmetries O_h , C_{4v} , and C_{3v} . Analysis including the higher levels, where more detailed experimental information is available,³ will be published in a subsequent paper.

In recent papers^{6,7} published by our group, it was shown that in the case of Gd^{3+} in CaF_2 , the crystal field parameters should have different values for energy levels with different J manifolds in order to obtain a reasonable fit with experiment. This means that crystal field theory, assuming the ligands as point charges, will not fully apply to the $CaF_2: Gd^{3+}$ system. The present investigation will show, however, that in contrast to the $CaF_2: Gd^{3+}$ case, crystal field theory will be applicable in the case of Sm^{3+} in CaF_2 , at least in the energy region up to $11\,000\text{ cm}^{-1}$ where 12 different J manifolds are involved.

II. EXPERIMENTAL

The crystals used in the present work were $CaF_2: Sm^{3+}$ single crystals supplied by the Harshaw Chemical Co. The Sm^{3+} concentration was 0.2% in these samples.

Absorption measurements were carried out in a Cary model 14 spectrophotometer with the crystals cut into platelets (approximately of $5 \times 8 \times 2\text{ mm}$ size) and held in the crystal holder of an Andonian custom-made vacuum cryostat. The tail of the cryostat was adapted to fit the sample compartment of the spectrophotometer. All measurements were carried out with the crystal at 77°K .

Figure 1 is a low-resolution (about 25 Å) absorption spectrum of the $CaF_2: Sm^{3+}$ crystal in the $9000\text{--}17000\text{ Å}$ region.

In the figure the peaks are numbered for purposes of identification, and their wavelengths and photon energies are given in Table I.

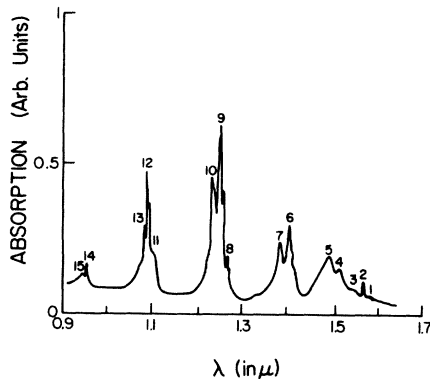


FIG. 1. Low-resolution absorption spectrum exhibited by Sm^{3+} in CaF_2 at 77°K .

TABLE I. Experimental energy levels of Sm^{3+} in CaF_2 (see Fig. 1).

	λ in Å	Energy in cm^{-1}
1	15 730	6357
2	15 665	6383
3	15 450	6472
4	15 085	6629
5	14 860	6730
6	13 980	7153
7	13 700	7257
8	12 615	7927
9	12 440	8039
10	12 268	8151
11	10 970	9116
12	10 825	9238
13	10 730	9320
14	9 505	10 521
15	9 425	10 610

III. CALCULATIONS

The crystal field potential for the five f electrons of the Sm^{3+} ion (f^5 configuration) in CaF_2 may be expanded in terms of tensor operators $C_q^{(k)}$,

$$V = \sum_i \left(\sum_{k,q} B_q^{(k)} C_q^{(k)} \right)_i, \quad (1)$$

where i runs over the five f electrons. This potential has the following explicit forms for the Sm^{3+} ion with O_h (octahedral), C_{4v} (tetragonal), and C_{3v} (trigonal) site symmetries in the CaF_2 matrix:

$$V(O_h) = \sum_i \left\{ B_0^{(4)} \left[C_0^{(4)} + \left(\frac{5}{14} \right)^{1/2} (C_4^{(4)} + C_{-4}^{(4)}) \right] \right. \\ \left. + B_6^{(6)} \left[C_0^{(6)} - \left(\frac{7}{2} \right)^{1/2} (C_4^{(6)} + C_{-4}^{(6)}) \right] \right\}_i, \quad (2)$$

where

$$B_0^{(4)} = B_0^{(4)} = \left(\frac{5}{14} \right)^{-1/2} B_4^{(4)},$$

$$B_6^{(6)} = B_0^{(6)} = - \left(\frac{7}{2} \right)^{-1/2} B_4^{(6)},$$

$$V(C_{4v}) = \sum_i \left[B_0^{(2)} C_0^{(2)} + B_0^{(4)} C_0^{(4)} + B_4^{(4)} (C_4^{(4)} + C_{-4}^{(4)}) \right. \\ \left. + B_0^{(6)} C_0^{(6)} + B_4^{(6)} (C_4^{(6)} + C_{-4}^{(6)}) \right]_i, \quad (3)$$

$$V(C_{3v}) = \sum_i \left[B_0^{(2)} C_0^{(2)} + B_0^{(4)} C_0^{(4)} + B_3^{(4)} (C_{-3}^{(4)} - C_3^{(4)}) \right. \\ \left. + B_0^{(6)} C_0^{(6)} + B_3^{(6)} (C_{-3}^{(6)} - C_3^{(6)}) \right. \\ \left. + B_6^{(6)} (C_{-6}^{(6)} + C_6^{(6)}) \right]_i. \quad (4)$$

Therefore we are to determine two B parameters in the case of O_h symmetry, five for C_{4v} , and six for C_{3v} symmetries.

Let

$$\phi_J(\mathcal{LS}) = \sum_{\alpha LS} U_{J\mathcal{LS}}(\alpha LS) \phi^0(\alpha LS)$$

be the free-ion wave function (intermediate-coupling state) with eigenvalue $E_J(\mathcal{LS})$. Here $(J\mathcal{LS})$ is a set of quantum numbers specifying an intermediate-coupling state, the ϕ^0 's are the pure LS basis states, and $U_{J\mathcal{LS}}(\alpha LS)$ represents the unitary matrix which diagonalizes the free-ion Hamiltonian. In this representation we can write the matrix element of the crystal field potential (1) using the standard tensor operator method in the form

$$V(JM\mathcal{LS}; J'M'\mathcal{L}'S')$$

$$= \sum_{k,q} B_q^{(k)} F_q^k(JM; J'M') G^k(J\mathcal{LS}; J'\mathcal{L}'S'), \quad (5)$$

where

$$F_q^k(JM; J'M') = (3 \parallel C^{(k)} \parallel 3) (-1)^{J-M} \begin{pmatrix} J & k & J' \\ -M & q & M' \end{pmatrix}, \quad (6)$$

$$G^k(J\mathcal{LS}; J'\mathcal{L}'S') = \sum_{\alpha\alpha' L'L'S} U_{J\mathcal{LS}}^*(\alpha LS) U_{J'\mathcal{L}'S'}(\alpha' L'S') \times (\alpha SLJ \parallel U^{(k)} \parallel \alpha' SL'J'). \quad (7)$$

Detailed descriptions of the above notations in (6) and (7) are given in Wybourne.⁸ By writing the matrix element in this form, the function $F_q^k(JM; J'M')$ on the right-hand side of (5) is M dependent and also symmetry dependent. On the other hand, the functions $G^k(J\mathcal{LS}; J'\mathcal{L}'S')$ represent M - and symmetry-independent matrices and are obtained by transforming the reduced matrices $(\alpha SLJ \parallel U^{(k)} \parallel \alpha' SL'J')$ by the unitary matrix $U_{J\mathcal{LS}}(\alpha LS)$. Once the matrices represented by (7) are obtained, they can be used for calculating energy levels of Sm^{3+} in CaF_2 with any symmetry within the f^5 configuration.⁹

The determination of the crystal field parameters requires the knowledge of the intermediate-coupling states and their eigenvalues. Fortunately, Carnall and his co-workers⁴ have calculated the free-ion energy states¹⁰ for most of the trivalent rare-earth ions. The usefulness of these in the study of crystal field splittings has been proved in the $\text{CaF}_2:\text{Gd}^{3+}$ system.⁷ Therefore we have used the free-ion eigenvectors of the Sm^{3+} ion calculated by Carnall *et al.*^{4, 11}

The reduced matrix elements $(\alpha SLJ \parallel U^{(k)} \parallel \alpha' SL'J')$ in (7) can be taken from Nielson and Koster¹² or can be calculated by the method of fractional parentage.¹³ We have calculated $(\alpha SLJ \parallel U^{(k)} \parallel \alpha' SL'J')$ using the coefficients of fractional parentage (CFP) of the f^5 configuration (taken from Nielson and Koster).¹²

Group-theoretical considerations reduce considerably the sizes of the Hamiltonian matrices. There are 12 different $(J\mathcal{LS})$ states in the energy region of our present interest. Since, for each one of 12 $(J\mathcal{LS})$ states, there are $(2J+1)$ degenerate $(JM\mathcal{LS})$ states, the total number of $(JM\mathcal{LS})$ basis states is 108, as shown in Table II. The set of $(2J+1)$ states for each J , however, forms a basis set of irreducible representations of the point group to which the site symmetry of Sm^{3+} ion in CaF_2 belongs. Decomposition of the set of $(2J+1)$ states for each J into the irreducible representations of the O_h , C_{4v} , and C_{3v} point groups are also shown in Table II. Accordingly, the sizes of the Hamiltonian matrices to be diagonalized are two 9×9 (Γ_6 and Γ_7) and one 18×18 (Γ_8) in the case of O_h symmetry, two 27×27 (Δ_6 and Δ_7) in C_{4v} , and one 36×36 (Γ_4) and one 18×18 ($\Gamma_5 + \Gamma_6$)¹⁴ in C_{3v} .

As usual, we define the rms deviation δ of calculated energy levels by

$$\delta = [\sum_i (E_{\text{expt}}^i - E_{\text{theor}}^i)^2 / (m - N)]^{1/2}, \quad (8)$$

where E_{expt}^i is the i th of the experimentally known levels, E_{theor}^i is the corresponding level obtained theoretically, m is the number of known levels, and N is the number of the $B_q^{(k)}$ parameters introduced in the Hamiltonian and is equal to 2, 5, and 6 in the case of O_h , C_{4v} , and C_{3v} symmetries, respectively. We attempted to determine a set of the $B_q^{(k)}$ parameters for each symmetry considered so as to minimize the rms deviation defined by (8).

IV. RESULTS AND DISCUSSIONS

The results of our calculations for Sm^{3+} in CaF_2 with O_h and C_{3v} site symmetries are given in Figs. 2 and 3 along with the experimental Stark components and the free-ion levels. Figure 2 shows the gross features of the set of energy levels lying in the energy region of interest (compare to Fig. 1). In Fig. 3 more detailed comparison between the calculated and experimental Stark split levels is presented. In Tables III and IV we list the numerical values of the calculated Stark components and the irreducible representations of the respective point groups to which they belong. Results for C_{4v} symmetry are not presented as we could not fit our calculated levels to experiment within reasonable agreement. (The rms deviation in this case was about 180 cm^{-1} .)

We obtained the following crystal field parameters and rms deviations for Sm^{3+} occupying O_h and C_{3v} sites in CaF_2 lattice:

$$O_h: B^{(4)} = -906 \text{ cm}^{-1}, \quad B^{(6)} = 618 \text{ cm}^{-1}, \\ \text{rms deviation} = 48.1 \text{ cm}^{-1}. \quad (9)$$

TABLE II. Decomposition of intermediate-coupling manifolds into irreducible representations of point groups O_h , C_{4v} , and C_{3v} .

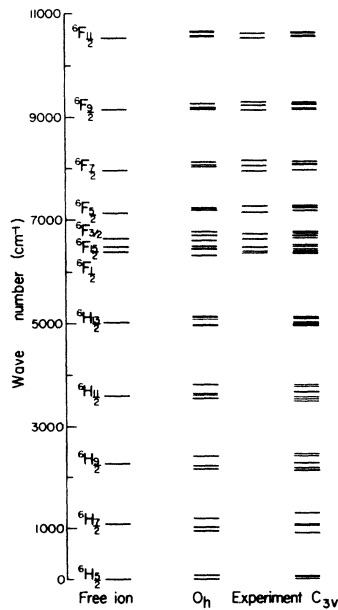
$J \mathcal{L} S^b$	$E_J (\mathcal{L} S)^c$	$2J+1$	Decomposition into irreducible representations of the point group ^a		
			O_h	C_{4v}	C_{3v}
${}^6H_{5/2}$	0	6	$\Gamma_7 + \Gamma_8$	$\Delta_6 + 2\Delta_7$	$2\Gamma_4 + (\Gamma_5 + \Gamma_6)^d$
${}^6H_{7/2}$	1038	8	$\Gamma_6 + \Gamma_7 + \Gamma_8$	$2\Delta_6 + 2\Delta_7$	$3\Gamma_4 + (\Gamma_5 + \Gamma_6)$
${}^6H_{9/2}$	2253	10	$\Gamma_6 + 2\Gamma_8$	$3\Delta_6 + 2\Delta_7$	$3\Gamma_4 + 2(\Gamma_5 + \Gamma_6)$
${}^6H_{11/2}$	3592	12	$\Gamma_6 + \Gamma_7 + 2\Gamma_8$	$3\Delta_6 + 3\Delta_7$	$4\Gamma_4 + 2(\Gamma_5 + \Gamma_6)$
${}^6H_{13/2}$	5014	14	$\Gamma_6 + 2\Gamma_7 + 2\Gamma_8$	$3\Delta_6 + 4\Delta_7$	$5\Gamma_4 + 2(\Gamma_5 + \Gamma_6)$
${}^6F_{1/2}$	6376	2	Γ_6	Δ_6	Γ_4
${}^6H_{15/2}$	6485	16	$\Gamma_6 + \Gamma_7 + 3\Gamma_8$	$4\Delta_6 + 4\Delta_7$	$5\Gamma_4 + 3(\Gamma_5 + \Gamma_6)$
${}^6F_{3/2}$	6620	4	Γ_8	$\Delta_6 + \Delta_7$	$\Gamma_4 + (\Gamma_5 + \Gamma_6)$
${}^6F_{5/2}$	7112	6	$\Gamma_7 + \Gamma_8$	$\Delta_6 + 2\Delta_7$	$2\Gamma_4 + (\Gamma_5 + \Gamma_6)$
${}^6F_{7/2}$	7960	8	$\Gamma_6 + \Gamma_7 + \Gamma_8$	$2\Delta_6 + 2\Delta_7$	$3\Gamma_4 + (\Gamma_5 + \Gamma_6)$
${}^6F_{9/2}$	9121	10	$\Gamma_6 + 2\Gamma_8$	$3\Delta_6 + 2\Delta_7$	$3\Gamma_4 + 2(\Gamma_5 + \Gamma_6)$
${}^6F_{11/2}$	10 506	12	$\Gamma_6 + \Gamma_7 + 2\Gamma_8$	$3\Delta_6 + 3\Delta_7$	$4\Gamma_4 + 2(\Gamma_5 + \Gamma_6)$
Total		108	$9\Gamma_6 + 9\Gamma_7 + 18\Gamma_8$	$27\Delta_6 + 27\Delta_7$	$36\Gamma_4 + 18(\Gamma_5 + \Gamma_6)$

^aNotations for various irreducible representations are consistent with those given by Koster (Ref. 13).

^bIntermediate-coupling (free-ion) state.

^cEigenvalue of intermediate-coupling state.

^d Γ_5 and Γ_6 form Kramer's pair.



$$C_{3v}: B_0^{(2)} = 118 \text{ cm}^{-1}, B_0^{(4)} = -272 \text{ cm}^{-1},$$

$$B_3^{(4)} = -296 \text{ cm}^{-1},$$

$$B_0^{(6)} = 38 \text{ cm}^{-1}, B_4^{(6)} = -128 \text{ cm}^{-1}, B_6^{(6)} = 1556 \text{ cm}^{-1},$$

TABLE III. Crystal field energy levels of Sm^{3+} in CaF_2 assuming O_h site symmetry. [Number of experimental levels^a = 15 (14); rms deviation^a = 48.1 (39.6) cm^{-1} .]

$J\mathcal{L}\mathcal{S}^b$	$E_J(\mathcal{L}\mathcal{S})^c$	Calculated Stark components	Experimental Stark components	Representa- tion ^d
${}^6H_{5/2}$	0	0 75		Γ_8 Γ_7
${}^6H_{7/2}$	1038	944 1016 1201		Γ_6 Γ_7 Γ_8
${}^6H_{9/2}$	2253	2175 2257 2418		Γ_6 Γ_8 Γ_8
${}^6H_{11/2}$	3592	3527 3650 3672 3789		Γ_8 Γ_6 Γ_8 Γ_7
${}^6H_{13/2}$	5014	4966 4986 5096 5123 5140		Γ_8 Γ_7 Γ_8 Γ_6 Γ_7
${}^6F_{1/2}$	6373 ^e	6331	6357	Γ_8
${}^6H_{15/2}$	6485	6420 6495 6590 6619 6696	6384 6472 6629 6730	Γ_6 Γ_6 Γ_8 Γ_8 Γ_7
${}^6F_{3/2}$	6620	6767		Γ_8
${}^6F_{5/2}$	7112	7192 7245	7153 7257	Γ_7 Γ_8
${}^6F_{7/2}$	7960	8027 8058 8115	(7927) 8039 8151	Γ_8 Γ_7 Γ_6
${}^6F_{9/2}$	9121	9169 9191 9255	9116 9238 9319	Γ_6 Γ_8 Γ_8
${}^6F_{11/2}$	10 506	10 599 10 561 10 622 10 630	10 521 10 610	Γ_7 Γ_8 Γ_8 Γ_6

^aSee discussions in text.

^bIntermediate-coupling (free-ion) state.

^cEigenvalue of intermediate-coupling state.

^dNotations for irreducible representations are consistent with those given by Koster (Ref. 13).

^eSee discussions in text.

TABLE IV. Crystal field energy levels of Sm^{4+} in CaF_2 assuming C_{3v} site symmetry. (Number of experimental levels = 15; rms deviation = 35.4 cm^{-1} .)

$J\mathcal{L}\mathcal{S}^a$	$E_J(\mathcal{L}\mathcal{S})^b$	Calculated Stark components	Experimental Stark components	Representa- tion ^c
${}^6H_{5/2}$	0	0 24 30		Γ_4 ($\Gamma_5 + \Gamma_6$) ^d Γ_4
${}^6H_{7/2}$	1038	891 1058 1064 1304		Γ_4 Γ_4 ($\Gamma_5 + \Gamma_6$) Γ_4
${}^6H_{9/2}$	2253	2133 2199 2275 2413 2462		Γ_4 ($\Gamma_5 + \Gamma_6$) Γ_4 ($\Gamma_5 + \Gamma_6$) Γ_4
${}^6H_{11/2}$	3592	3481 3516 3559 3691 3751 3775		Γ_4 ($\Gamma_5 + \Gamma_6$) Γ_4 Γ_4 ($\Gamma_5 + \Gamma_6$) Γ_4
${}^6H_{13/2}$	5014	4963 4969 4970 5010 5102 5121 5127		Γ_4 Γ_4 ($\Gamma_5 + \Gamma_6$) Γ_4 Γ_4 ($\Gamma_5 + \Gamma_6$) Γ_4
${}^6F_{1/2}$	6373 ^e	6360	6357	($\Gamma_5 + \Gamma_6$)
${}^6H_{15/2}$	6485	6369 6384 6418 6490 6518 6651 6698 6725	 6384 6472 6629 6730	Γ_4 Γ_4 ($\Gamma_5 + \Gamma_6$) Γ_4 Γ_4 Γ_4 ($\Gamma_5 + \Gamma_6$) Γ_4
${}^6F_{3/2}$	6620	6750 6761		($\Gamma_5 + \Gamma_6$) Γ_4
${}^6F_{5/2}$	7112	7193 7248 7277	7153 7257	Γ_4 ($\Gamma_5 + \Gamma_6$) Γ_4
${}^6F_{7/2}$	7960	7956 8082 8088 8121	7927 8039	Γ_4 ($\Gamma_5 + \Gamma_6$) Γ_4 Γ_4
${}^6F_{9/2}$	9121	9126 9164 9248 9264 9276	9116 9238 9319	Γ_4 ($\Gamma_5 + \Gamma_6$) Γ_4 ($\Gamma_5 + \Gamma_6$) Γ_4

$$\text{rms deviation} = 35.4 \text{ cm}^{-1}. \quad (10)$$

In the case of O_h symmetry, fitting to a particular

TABLE IV. (continued)

$J\mathcal{L}\mathcal{S}^a$	$E_J(\mathcal{L}\mathcal{S})^b$	Calculated Stark components	Experimental Stark components	Representa- tion ^c
${}^6F_{11/2}$	105 06	105 59	10 521	Γ_4
		105 76		$(\Gamma_5 + \Gamma_6)$
		105 83		Γ_4
		105 92		Γ_4
		106 14	10 610	$(\Gamma_5 + \Gamma_6)$
		106 27		Γ_4

^aIntermediate-coupling (free-ion) state.^bEigenvalue of intermediate-coupling state.^cNotations for irreducible representations are consistent with those given by Koster (Ref. 13).^d Γ_5 and Γ_6 form Kramer's pair.^eSee discussions in text.

level at 7927 cm^{-1} which belongs to the ${}^6F_{7/2}$ multiplet was not good in all stages of the iteration. If we omit this level from our calculation, then the rms deviation reduces to 39.6 cm^{-1} .

It is quite possible that there exist two types of Sm^{3+} ion sites in the CaF_2 lattice simultaneously, one with O_h symmetry and the other with C_{3v} symmetry. If the charge compensator is far from the Sm^{3+} ion, the local symmetry around Sm^{3+} will be O_h . The C_{3v} site symmetry will be achieved by a charge compensator replacing one of the eight F^- ions nearest to the Sm^{3+} ion. The charge compensator in this case will most probably¹⁵ be in an "as-received" crystal the OH^- complex. As discussed in the Introduction, by studying effects of heat treatment, one is able to obtain the information³ about the "symmetry development" of the rare-earth ion site. Unfortunately this type of study is not practical for absorption lines in the present region of interest. Furthermore, the optical resolution achieved by the spectrophotometer in this wavelength region is relatively poor. This fact may mean that not all Stark components present in a given manifold will actually be resolved. Hence one will not be able to determine beyond reasonable doubt the site symmetry responsible for the given spectra. In fact, the rms deviations of the calculated levels for O_h and C_{3v} symmetries are both of the same order of magnitude, and it is difficult to say which symmetry is more suitable to interpret the experimental peaks. Rather, one may interpret the results in the following way: The fact that we obtained reasonable fits for both O_h and C_{3v} symmetries might be the consequence of the sample containing both types of Sm^{3+} sites, one with O_h symmetry and the other with C_{3v} symmetry. However, because of "poor" resolution, one is not able to resolve all Stark components.

In his study of the fluorescence spectra of Sm^{3+} in CaF_2 at tetragonal sites, Rabbiner² obtained the

calculated splitting of the ground state (${}^6H_{5/2}$ multiplet) to be of 223 cm^{-1} . Prener and Kingsley¹⁶ investigated the fluorescence spectra of Sm^{3+} in CdF_2 , which is isomorphous to CaF_2 , and gave the experimental values for the ground-state splitting of 147 cm^{-1} . They suggested that the splitting should be associated with a tetragonal field surrounding the Sm^{3+} ion in CdF_2 . In the present work we do not have direct information concerning the splittings of the ground state of Sm^{3+} in CaF_2 . Our calculated splittings of the ground state for O_h and C_{3v} symmetries, however, are 75 cm^{-1} and 30 cm^{-1} , respectively. In view of the rms deviations of our calculated levels, we feel that the splitting of the ground state in either case will be of about 100 cm^{-1} or less. Under those circumstances, then, the "upper" ground states will be sufficiently populated even at 77 °K to give absorption lines associated with them. Thus, each peak will be a composite peak composed of two lines, and of three lines for O_h and C_{3v} symmetries, respectively, making a detailed analysis of the absorption spectrum even more complicated. Studying the temperature variations and relative intensities of these components using high-resolution spectrometers might provide information concerning the ground-state splittings and site symmetries of the Sm^{3+} ion.

The results listed in Tables III and IV show that the absolute deviations of the calculated levels from the experimental ones are distributed rather randomly over the different J manifolds. In addition, the gross feature of the whole spectrum is represented fairly well by the calculations in both cases of O_h and C_{3v} symmetries (see Fig. 2). It should be noted here that the above results were obtained using a single set of crystal field parameters to describe the energy levels involving 12 different J manifolds. This, we suggest, means that crystal field theory with a single set of parameters "works" well in the $\text{CaF}_2 : \text{Sm}^{3+}$ systems at least in the energy region of the present interest. In the case of Gd^{3+} in CaF_2 , the situation is quite different, as was discussed in the Introduction. Probably this difference comes from the following two reasons: (i) In the present paper, we are only concerned with the low-lying levels up to 11 000 cm^{-1} . In the case of Gd^{3+} in CaF_2 , however, energies involved are much higher ranging from $\approx 32\,000$ to $\approx 37\,000$ cm^{-1} . (ii) There is a fairly large energy gap of ≈ 7500 cm^{-1} separating the low-lying levels from higher ones in the present case. There is no such gap in $\text{CaF}_2 : \text{Gd}^{3+}$ system.

Inspection of the eigenvectors obtained in our calculation shows that, in spite of working in the complete intermediate-coupling scheme, the J mixing effects are not too serious except for a group of levels ranging from ≈ 6300 to ≈ 6800 cm^{-1} . In other words, the total angular momentum J is still a rea-

sonably good quantum number to even specify the Stark split levels of Sm^{3+} except for the above mentioned levels. In this group of levels, which orig-

inates from three different J manifolds ${}^6F_{1/2}$, ${}^6H_{15/2}$, and ${}^6F_{3/2}$, the effect of J mixing is considerable, i.e., probably due to the closeness of these levels.

[†]Work supported by the National Research Council and the Defense Research Board of Canada.

*On leave from the Department of Physics, College of Arts and Sciences, Tohoku University, Sendai, Japan.

¹M. J. Weber and R. W. Bierig, Phys. Rev. **134**, A1492 (1964); R. W. Bierig, M. J. Weber, and S. I. Warshaw, *ibid.* **134**, A1504 (1964).

²N. Rabbiner, Phys. Rev. **130**, 502 (1963); J. Opt. Soc. Am. **57**, 1376 (1967).

³S. T. Pai, Ph.D. thesis, University of Windsor, 1970 (unpublished).

⁴W. T. Carnall, P. R. Fields, and K. Rajnak, J. Chem. Phys. **49**, 4424 (1968).

⁵Slightly deformed symmetries from pure O_h , C_{4v} and C_{3v} are also possible.

⁶M. Nerenberg and M. Schlesinger, Phys. Letters **26A**, 109 (1968); M. Schlesinger and M. Nerenberg, Phys. Rev. **178**, 568 (1969).

⁷M. A. H. Nerenberg, G. A. Behie, and M. Schlesinger, Phys. Letters **31A**, 212, (1970).

⁸B. G. Wybourne, *Spectroscopic Properties of Rare Earths* (Interscience, New York, 1965).

⁹If we are only interested in a certain energy range, then the sizes are even more reduced. For example, the sizes are only 12×12 in the energy region up to

$11\,000\text{ cm}^{-1}$ in which we are interested in the present paper.

¹⁰The vectors of Carnall *et al.* are not really for the free ion, but are instead vectors for aqueous solution involving some loosely bonded species. We also assume that the free-ion E_k and ζ values do not depend on coordination, environment, etc.

¹¹We are much indebted to Dr. W. T. Carnall for providing us with the detailed information about the free-ion energy states of the Sm^{3+} ion. Actually, we have recalculated the free-ion energy states of Sm^{3+} by employing the same parameters given by Carnall *et al.* (Ref. 4) in order to avoid the possibility of making trivial errors in transcribing the data.

¹²C. W. Nielson and G. F. Koster, *Spectroscopic Coefficients for p^n , d^n , and f^n Configurations* (MIT Press, Cambridge, Mass., 1964).

¹³G. F. Koster, in *Solid State Physics*, edited by F. Seitz and D. Turnbull (Academic, New York, 1957), Vol. 5.

¹⁴ Γ_5 and Γ_6 form Kramer's pair in the case of C_{3v} symmetry.

¹⁵J. Sierro, J. Chem. Phys. **34**, 2183, (1961).

¹⁶J. S. Prener and J. D. Kingsley, J. Chem. Phys. **38**, 667 (1963).

Positron Annihilation Rates in Lanthanum Hydrides[†]

Richard Green* and William G. Bos

Department of Chemistry, University of Louisville, Louisville, Kentucky 40208

and

W. F. Huang

Department of Physics, University of Louisville, Louisville, Kentucky 40208

(Received 1 June 1970)

Positron annihilation rates λ_1 and λ_2 are reported for a series of lanthanum hydride samples of compositions from $\text{LaH}_{2.0}$ to $\text{LaH}_{2.9}$. From $\text{LaH}_{2.0}$ to $\text{LaH}_{2.7}$, λ_1 was approximately constant at 3.36 nsec^{-1} . At higher compositions, λ_1 increased with increasing hydrogen content. A slower rate component λ_2 was observed for annihilation in lanthanum hydrides, but the associated intensity was very low. New data are also reported for lithium hydride as follows: $\lambda_1 = 3.12\text{ nsec}^{-1}$, $\lambda_2 = 0.68\text{ nsec}^{-1}$, and $I_2 = 6.30\%$.

INTRODUCTION

Positron annihilation provides an attractive approach to the study of bonding in solids. Two types of measurements have been extensively used to characterize the annihilation process in solids: the measurement of positron lifetimes and the measurement of the two-photon angular correlations. Positronium formation is precluded in ionic solids.¹ The formation of a positron-anion bound

state remains a subject of discussion^{2,3} and has been most extensively treated for the case of the hydride ion. Gol'danski *et al.*⁴ treated a bound state consisting of a positron-hydride-ion pair in relation to the fast component of the lifetime spectrum of lithium hydride. Ivanovna and Prokop'ev⁵ attempted to account for additional lifetime components in lithium hydride in terms of additional excited states of this bound state. More recently,